

# Analysis and Parametric Modeling of RF MEMS Capacitive Shunt Switch

N. AbuGhalioun, H. Hassan, and H. Ibrahim  
Electronics and Communications Engineering  
Arab Academy for Science and Technology and Maritime Transport  
EGYPT

**Abstract:** - MEMS capacitive shunt switches with variable resonant frequencies are discussed in this paper. Advantages of such switches are low-loss performance ( $< 0.5\text{dB}$ ), high isolation ( $> 40\text{dB}$ ), High Capacitance ratio and ease of fabrication. The switches are placed over a  $45/60/45\text{ }\mu\text{m}$  copper CPW and a FEM simulation software (Ansoft HFSS) is used to extract the S-parameter for different switch geometries. An equivalent lumped circuit model is constructed from the S-parameters and different values of inductance are calculated. The capacitance of the switches in the down-state is around  $5.1\text{pF}$  and the inductances range from  $2\text{pH}$  to  $27\text{pH}$  which result in resonant frequency range of  $13\text{-}50\text{ GHz}$ . The mechanical model of the switch is discussed and calculations of different characteristics of the switch such as the pull-in voltage and spring constant are outlined.

**Key-Words:** - MEMS shunt switch, Electrostatic actuation, Low-loss, High isolation, Parametric model, Low spring constant

## 1 Introduction

MEMS switches were first introduced by Peterson in 1971 [1]. Since then, many MEMS switches have been reported with different geometries and characteristics such as low insertion loss and high isolation which are suitable for microwave applications [2-4]. These switches showed a better performance than conventional FETs and PIN switches specially when used in microwave applications. The resonant frequency of MEMS switches is controlled by its down capacitance ( $C_{\text{down}}$ ) and the parasitic inductance ( $L$ ) [7]. In this paper it is shown that the resonant frequency can be controlled by changing inductance of the switch using various geometries of the inductive meanders as shown in Table 2. To visualize the electromagnetic characteristics of the switch, a FEM simulator (Ansoft HFSS) that is based on full wave analysis was used. The resonant frequency and inductance were extracted from the scattering parameters. At the end of the paper, it is shown that by combining several switches one can achieve better performance in terms of isolation and bandwidth.

## 2 Device Structure

The switch under experiment was originally developed by the University of Michigan [4]. Fig.1 shows the structure of the switch and its physical dimensions are listed in Table.1. The switch is placed  $3\text{ }\mu\text{m}$  above a coplanar waveguide with dimensions  $(45/60/45\text{ }\mu\text{m})$ . Two actuation electrodes are placed under the supported membranes having an area of  $(190 \times 190\text{ }\mu\text{m}^2)$  each.

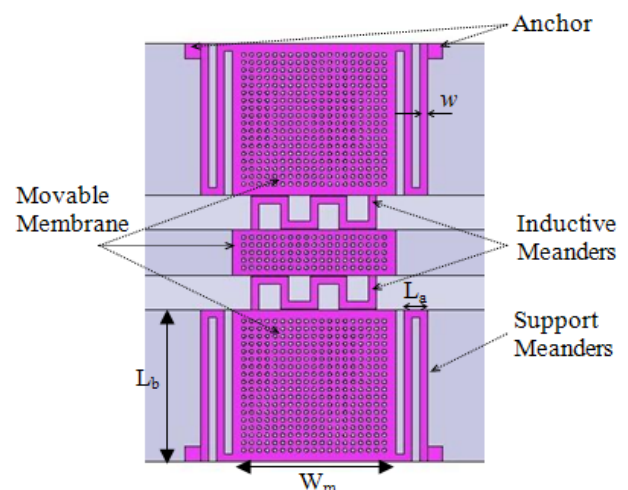


**Fig.1** Model of the capacitive MEMS switch over CPW line.

**Table 1** Physical dimensions of the MEMS switch.

$L_a$	20 $\mu\text{m}$
$L_b$	200 $\mu\text{m}$
$W_m$	210 $\mu\text{m}$
$w$	10 $\mu\text{m}$
Thickness ( $t$ )	2 $\mu\text{m}$
Material	Nickel
Mass	$2.16 \times 10^{-9}$ kg
Dielectric	$\text{Si}_3\text{N}_4$ ( $t_d = 0.15$ $\mu\text{m}$ )
Holes radius	2.5 $\mu\text{m}$

### 3 Mechanical Characteristics

The dynamic equation for motion of the switch is given by [5]:

$$m \frac{\partial^2 z}{\partial t^2} + b \frac{\partial z}{\partial t} + Kz = \frac{\epsilon_o A V^2}{2(g + \frac{t_d}{\epsilon_r} - z)^2} \quad (1)$$

where  $m$  is the mass of beam,  $b$  is the damping coefficient,  $K$  is the spring constant, and the right hand side of the equation is the electrostatic force due to actuation electrodes characterized by the actuation area  $A$  and voltage  $V$  applied on them,  $g$  is the initial gap height,  $\epsilon_o$  and  $\epsilon_r$  is the permittivity of air and the dielectric respectively, and  $t_d$  is the dielectric thickness.

Folded meanders are attached to the square plates responsible for the electrostatic actuation. The main purpose for these meanders is lowering the membrane's spring constant ( $k_z$ ). This meander geometry results in  $k_z$  approximated by [5]:

$$k_z = \frac{E w \left( \frac{t}{L_a} \right)^3}{1 + \frac{L_b}{L_a} \left( \left( \frac{L_b}{L_a} \right)^2 + 12 \frac{1 + \nu}{1 + \left( \frac{w}{t} \right)^2} \right)} \quad (2)$$

where  $E$  and  $\nu$  are the Young's modulus and the Poisson's ratio of the metal (200 GPa and 0.31 respectively for Nickel). The sum of spring constants at all meanders results in the total spring constant ( $K$ ) which is equal to:

$$K = \frac{4k_z}{N} \quad (3)$$

where  $N$  is the number of meanders at the suspension ( $N=2$  in this case). From the equation above it's clear that the spring constant decreases with increasing meander number.

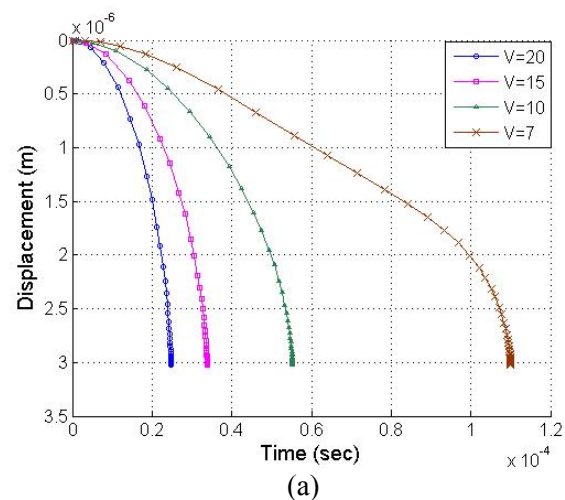
The voltage applied between the pull in electrode and actuation area of the membrane is a function of the spring constant derived previously and is usually  $(1.2-1.4) \times V_p$  where  $V_p$  is the pull-in voltage and is given by [2]:

$$V_p = \sqrt{\frac{8K_z g_o^3}{27A\epsilon_o}} \quad (4)$$

where  $g_o$  is the gap between the bridge and ground, and  $A$  is the actuation area.

It is tempting to increase the number of meanders so as to lower the spring constant and thereby lower  $V_p$ , but problems such as stiction could arise from such procedure [6].

Equation (1) was solved using MATLAB for different applied voltages. The time needed for the switch to move a distance of 3  $\mu\text{m}$  is shown in Fig.2 (a) for applied voltages of 7, 10, 15, and 20 volts. The switching time for the voltages applied is 110 $\mu\text{s}$ , 55.2 $\mu\text{s}$ , 33.8 $\mu\text{s}$ , and 24.7 $\mu\text{s}$  respectively. In Figure.2 (b) the applied voltage is less than the required pull-in voltage (6 volts) and hence the switch will not make it to the ground. Instead it will move for a short distance (about 0.8 $\mu\text{m}$ ) and then starts vibrating up and down for a while until it almost settles around 0.435 $\mu\text{m}$ . It should be noted that at  $V=7$  the switch took longer time to snap down. At this voltage the system is at the critical voltage (around  $V_p$ ) at which the switch could operate.



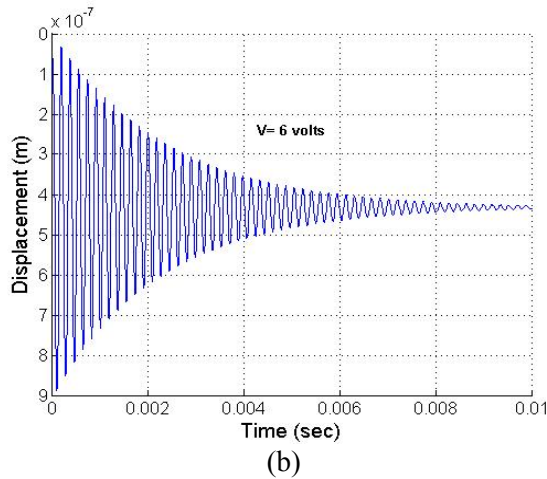


**Fig.2** Time vs. Displacement of the switch when the applied voltage is (a) greater than  $V_p$  ( $V= 7,10,15,20$  volts) and when it is (b) less than  $V_p$  ( $V= 6$  volts)

## 4 RF Characteristics

As mentioned earlier the switch was analyzed with a full-wave analysis simulation software (Ansoft HFSS) [8] when using different geometries of the inductive beams. In the up state position all the switches showed low insertion loss. The up-state capacitance ( $C_{up}$ ) is around 46 fF for all switches.

The resulting s-parameters showed different isolations and resonant frequencies as shown in Fig.3. They were fitted to get the inductance for each switch. Table.2 shows the values for  $f_r$  and  $L$  for each case. The down capacitance ( $C_{down}$ ) is the same for all switches (5.1 pF) and the capacitance ratio ( $C_{down}/C_{up}$ ) is 110:1. Where,

$$\frac{C_{down}}{C_{up}} = \frac{\epsilon_o \epsilon_r A}{t_d} \left( \frac{\epsilon_o A}{g + t_d / \epsilon_r} \right) + C_f \quad (5)$$

From Table 2 it is clear that the resonant frequency increases as the inductance decrease. By carefully controlling the width and shape of the meanders one can get maximum isolation at any desired resonant frequency.

**Table 2**  $f_r$  and  $L$  for 8 different inductive beams

Inductive Meander		$f_r$ (GHz)	$L$ (pH)
1		13.5	27.3
2		16	19.4
3		17	17.2
4		20	12.4
5		23.25	9.2
6		29	5.9
7		39.5	3.2
8		49.75	2

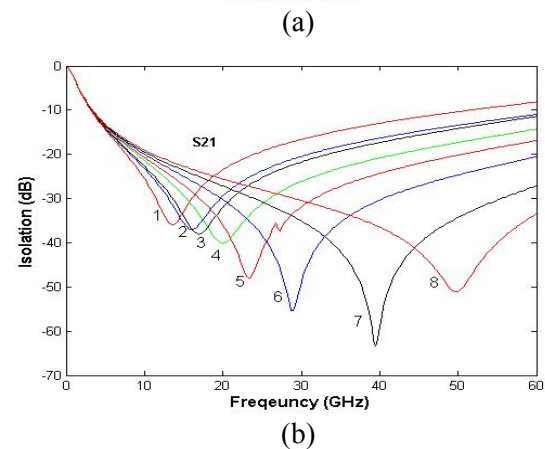
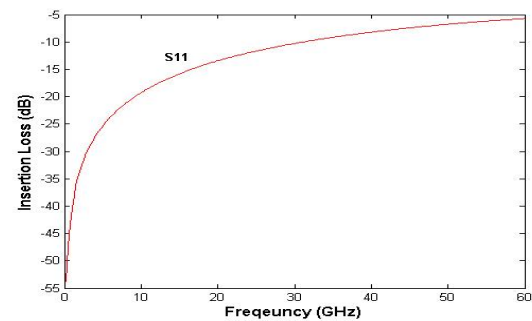


**Fig.3** (a) Insertion loss in up-state and (b) isolation in down-state for the switches. Numbers correspond to the inductive beams in Table 2

Inductive beams 1 and 2 have lengths 160  $\mu\text{m}$  and 120  $\mu\text{m}$  respectively and their width is 10  $\mu\text{m}$ . The length was fixed at 180  $\mu\text{m}$  for beams 3 and 4 and the width was changed to 15  $\mu\text{m}$  and 20  $\mu\text{m}$  respectively. Beams 5 and 6 are rectangular in shape having widths 10  $\mu\text{m}$  and 30  $\mu\text{m}$  respectively. For beams 7 and 8 three rectangular shaped beams were used with fixed width of 10  $\mu\text{m}$  while varying the distance between them to 30  $\mu\text{m}$  and 60  $\mu\text{m}$  respectively.

## 5 Parallel switches

Higher isolation and wider bandwidth greater than the ones of a single switch is sometimes required by applications. To accomplish this, several switches with different inductances could be connected in parallel. Fig.4 illustrates the layout of the switches over the CPW and their RF characteristics are shown in Fig.5. Four switches using the inductive beams 1 to 4 from Table.2 were used. The simulation results showed isolation higher than 60 dB between 15 and 45 GHz. The simulation resulted in isolation greater than 90dB at 15 GHz but it is expected that the actual isolation will be lower than the one obtained. Yet previous measurements of similar switches [7] showed that the isolation will be greater than 40 dB for the range of frequencies stated above.

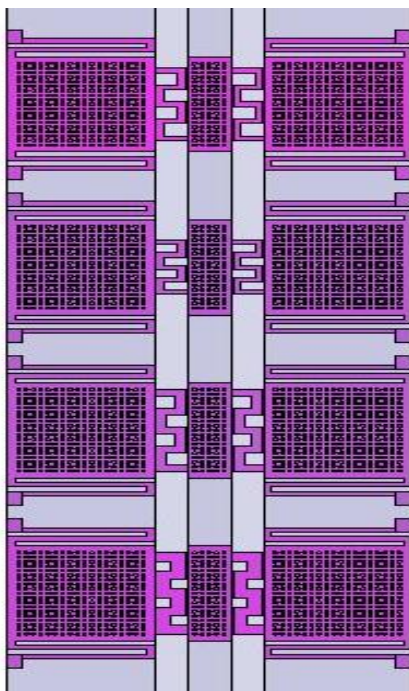


Fig.4 Four switches in Parallel.

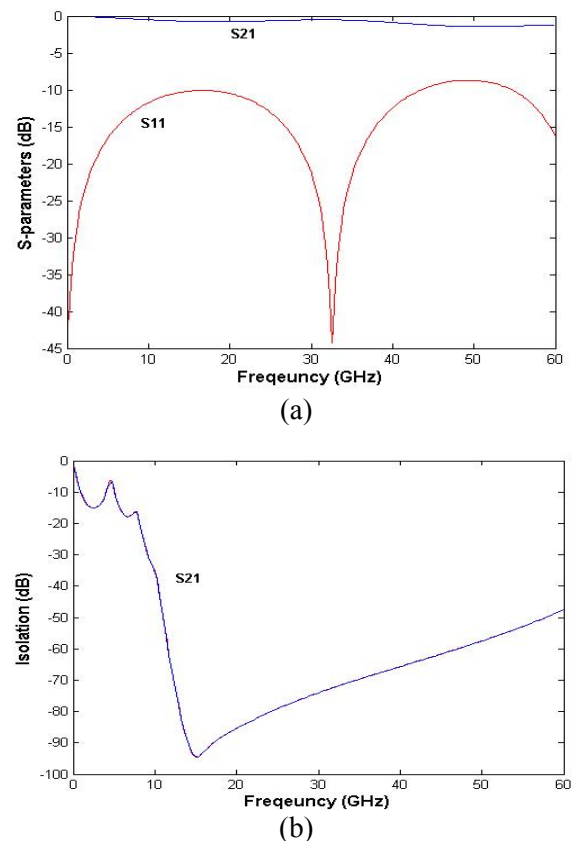


Fig.5 Simulated results for the parallel switches in (a) the up-state and (b) down-state

## 6 Conclusion

The implementation of different geometries of inductive meanders was demonstrated to design resonant switches. The simulation results showed high isolation, low insertion loss, and low pull-in voltage. Single switches can be used to selectively isolate a preferred frequency or in a network to get maximum isolation over a wide range of frequencies. Different applications such as tunable filters can benefit from these types of switches.

### References:

- [1] K. E. Petersen, "Micromechanical membrane switches on silicon", IBM Journal of Research and Development, vol. 23, pp. 376-385, July 1971.
- [2] Gabriel M. Rebeiz, "RF MEMS, Theory, Design, and Technology", New York: Wiley, 2003

[3] C. L. Goldsmith, Z. Yao, S. Eshelman, and D. Denniston, "*Performance of low-loss RF MEMS capacitive switches*", IEEE Microwave and Guided Wave Letters, vol. 8, pp. 269-271, Aug., 1998.

[4] Sergio P. Pacheco, Linda P. B. Katehi, and Clark T.-C. Nguyen, "*Design of Low Actuation Voltage RF MEMS Switch*", Microwave Symposium Digest., 2000 IEEE MTT-S International, 11-16 June 2000 pp.165 - 168 vol.1

[5] Fedder G K 1994 "*Simulation of microelectro-mechanical systems*" Ph.D. dissertation Dept. Elect. Eng. Comput. Sci., (Univ. California at Berkeley, Berkeley, CA).

[6] Peroulis, D.; Pacheco, S.P.; Sarabandi, K.; Katehi, "*Electromechanical considerations in developing low-voltage RF MEMS switches*", L.P.B.; Microwave Theory and Techniques, IEEE Transactions on Volume 51, Issue 1, Part 2, Jan. 2003 pp.259 – 270

[7] Peroulis, D.; Pacheco, S.; Sarabandi, K.; Katehi, P.B.; "*MEMS devices for high isolation switching and tunable filtering*", Microwave Symposium Digest., 2000 IEEE MTT-S International, 11-16 June 2000 pp.1217 - 1220 vol.2

[8] High Frequency Structure Simulation, (Ansoft HFSS) Version 9.0, Ansoft Inc.